ISSN 2616-5872 Vol.6, Issue 5: 12-22, DOI: 10.25236/AJEE.2024.060503

Design of pulse pattern based on the theory of linear congruence for BeiDou pseudolite signals

Fusheng Wei[1], Di Wu[2]

[1]*Guangdong Environmental Protection Engineering Vocational College, Foshan, Guangdong, 528216, China*
[2]*Key Laboratory of Environment Change and Resources Use in Beibu Gulf, (Nanning Normal University), Ministry of Education, Nanning, Guangxi, 530001, China*

Abstract: *BeiDou pseudolites are ground-based BeiDou-like signals transmitters to augment positioning accuracy and service availability of the BeiDou satellite navigation system. A significant challenge − the "near far problem" arises because sometimes the signals from the nearby BeiDou pseudolites are strong enough to block the satellite signals. One of the promising solutions is to pulse the pseudolite signals with a low duty cycle to reduce the interference. Some existing pulsing schemes, i.e., the RTCM SC-104 and the RTCA SC-159 have been proved effective in many applications. However, most of them are unable to provide a close, multiple pseudolite transmissions due to the random pulse pattern. In this paper, a pseudo-random pulse pattern based upon the theory of linear congruence has been proposed to improve the multi-access performance. The spectral and temporal characteristics of the proposed pulse pattern are analyzed and compared with the random pulse pattern. From the analysis, it emerges that the proposed scheme features better characteristics to facilitate multiple pseudolite transmission.*

Keywords: *BeiDou pseudolite, pulsed signal, duty cycle, near-far problem, linear congruence*

1. Introduction

Being ground-based navigation signal transmitters, pseudolites (PLs) are set to compliment the global navigation satellite system (GNSS) constellations if there are insufficient observable satellites, such as in an urban canyon or a deep open mine [1-3]. Implementation of PLs has been endorsed in many modernization programs of GNSS, such as the Aeronautical Radio Navigation Service[4] for the GPS the "Local Elements" [5] for the Galileo system. The Chinese BeiDou system is currently in the process of constellation construction, implementation of the BeiDou pseudolites has also been proposed to augment the signal coverage and positioning precision.
In practical PLs deployment, the "near-far problem" is one of the severe challenges that must be overcome. For maximum compatibility, most PLs broadcast in the GNSS bands, introducing additional interference to the satellite signal acquisition. Compared with the received satellite signal power which is nearly constant, the PL signal power varies greatly in accordance with the distance from the user on the ground. At the "near" point, the received PL signal power is strong enough to saturate the receiver and in fact disable the satellite signal detection [6].

There are many solutions have been adopted to reduce the interference, in which signal pulsing the most popular one [7]. By transmitting a small portion of the entire period signal with a low duty-cycle pulse, the interference can be averaged to an acceptable level. For example, the Radio Technical Commission for Maritime Services (RTCM) SC-104 scheme [8] was designed for the GPS PLs where a 1023 chips code is transmitted in 11 pulses of 93 chips each, so that the average interference time is 10% of the code period, which is acceptable for the receiver to track both satellite and PLs signal. However, the RTCM SC-104 scheme employs a random pulse position arrangement mechanism, results in a high pulse collision probability especially when multiple PLs are applied. Therefore, the RTCM SC-104 scheme is not the optimal option for the BeiDou PL implementation.

Pseudo-random sequences have found several applications in the communications field for the design of frequency hopping sequences where the signal transmission orders are arranged in the pseudo-random way to avoid the interference in the frequency division multi-access (FDMA) system. The linear congruence theory is the most widely used pseudo-random sequence generation method which has been proved effective in the Radar and Sonar signal design. In this paper, the BPL pulsing

ISSN 2616-5872 Vol.6, Issue 5: 12-22, DOI: 10.25236/AJEE.2024.060503

scheme based upon the linear congruence theory was designed and analyzed. This paper is organized as follows: first an overview of the pulsing scheme models is presented. Pulse pattern construction based on both random theory and the linear congruence theory are introduced in section 3. Signal characteristics analysis and comparison between the two types of patterns are conducted in section 4. Conclusion is made in Section 5.

2. Pulsing scheme model and parameters

The signal transmitted by the BeiDou PL is composed of two components:

$$S_{PL}[n] = S[n] \cdot P[n] \tag{1}$$

where $S[n]$ is the ranging code which can be used to compute the pseudo-range, $P[n]$ is the high energy pulses for long haul transmission. Same as the satellite signal, the PL ranging code is comprised of Gold code with length $N_c = 2046$ and quadrature phase shift keying subcarriers. Different phase shifts are assigned to the PL ranging code to sustain the orthogonality required by the interoperability between BeiDou satellites and PLs. The pulse component can be expressed as:

$$P[n] = \sum_{-\infty}^{+\infty} P_b[n - iN_e \cdot N_c] \tag{2}$$

where $P[n]$ can be seen as the repetition of the basic pulse pattern $P_b[\cdot]$ which is a set of sequence that define the transmission time slots, N_e is the number of the code period repetitions within the basic pulse pattern. The length of the basic pulse pattern can be obtained by $T_e = N_e \cdot N_c \cdot T_{ch} = N_e \cdot T_c$, where T_{ch} is the duration of one single chip. The model that characterize the pulsing scheme is illustrated in Fig.1.

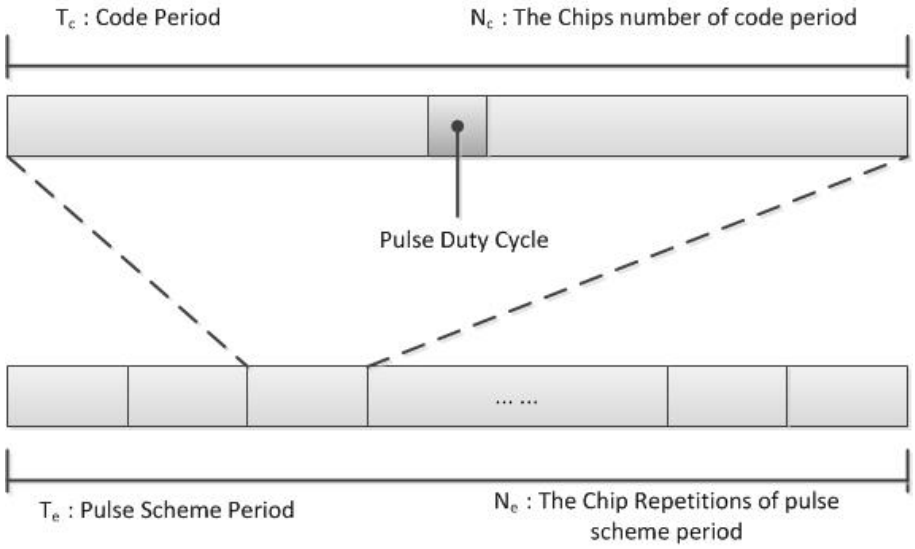

Figure 1: A schematic diagram of parameter relation of pulse modulation scheme

Pulse duty cycle is the most important parameter, not only it determines the pulse duration but the pulsing scheme period. It can be expressed as:

$$d = \frac{1}{N_e N_c} \sum_{n=0}^{N_e N_c - 1} P_b[n] \tag{3}$$

where $\frac{1}{N_e N_c}$ denotes the average pulse duration of the entire pulsing scheme. (3) can be further expressed as:

$$d = \frac{1}{N_e} \sum_{n=0}^{N_e - 1} d_k \tag{4}$$

where d_k is the duty cycle of one code period:

$$d_k = \frac{1}{N_c} \sum_{n=0}^{N_c} P_b[n + kN_c] \tag{5}$$

It is desirable to have a uniform pulse scheme that $d = d_k$ to preserve the autocorrelation function of the pulsed signal. For example, when $d_k = 6.25\%$, one can transmit 2046 chips in $N_e = (1/d_k) =$

ISSN 2616-5872 Vol.6, Issue 5: 12-22, DOI: 10.25236/AJEE.2024.060503

16 code period, in which the entire duty cycle $d = d_k = 6.25\%$. On the other hand, if $d_k = 6\%$, the transmission period is $N_e = (1/d_k) + 1 = 17$, it turns out that $d = 5.88$. Therefore, a careful duty cycle consideration is required.

Assuming that only one pulse is transmitted in each code period, the basic pulse pattern can be expressed as:

$$P_b[n] = \sum_{k=0}^{N_e-1} \Pi_{d_i N_c}[n - kN_c - \tau_k] \tag{6}$$

where τ_i denotes the time slot assigned to the ith pulse, $\Pi_{d_k N_c}[n]$ represents the rectangular wave of the pulse with the duration of $d_k N_c$ the:

$$\Pi_{d_k N_c}[n] = \begin{cases} 1, & \text{n} = 0,1,2 \dots \dots d_k N_c - 1; \\ 0, & \text{else} \end{cases} \tag{7}$$

if $d_k = d$, (7) can be rewritten as:

$$P_b[n] = \sum_{k=0}^{N_e-1} \Pi_{dN_c}[n - kN_c - \tau_k] \tag{8}$$

where$\tau_k \in \{1,2,3, \dots \dots, N_e\}$. The basic pulse pattern is characterized by the pulse duration $d_k N_c$ and transmission time-slots arrangement. Consequently, design of a pulsing scheme relies on the construction of the pulse pattern.

3. Pulse pattern construction

3.1 Random permutation pattern

The first step of pulse pattern construction is to break the code into several blocks with durations $\{d_k N_c\}_{k=0}^{N_e-1}$.For any type of the GNSS ranging code, equal duration is not the best option, because in some cases the pulse duration may not be a integer, which may cause some spectrum distortion of the ranging code. Thus, it is proposed that the pulse durations be chosen as follows:

$$\begin{aligned} d_n N_c &= \lfloor dN_c \rfloor \\ d_s N_c &= \lfloor dN_c \rfloor + 1 \end{aligned} \tag{9}$$

where $d_n N_c$ is the duration for normal pulses,$d_s N_c$is the duration for special pulses,the symbol $\lfloor \cdot \rfloor$ denotes the floor operation. The special pulse is one chip larger to contain the fractional part clipped by the floor operation, so that the duration variation can be averaged to the minimum. The full code can be transmitted in the minimum amount of time, corresponding to $N_e = N_n + N_s$ code periods.

$$d = \frac{1}{N_c + N_s} \tag{10}$$

Based on the fact that $N_n d_n N_c + N_s d_s N_c = N_c$, N_n and N_s can be obtained by:

$$\begin{aligned} N_s &= N_c - N_e d_n N_c \\ N_n &= N_e - N_s \end{aligned} \tag{11}$$

Consequently, the pulse durations $\{d_k N_c\}_{k=0}^{N_e-1}$ is the set

$$N_\tau = \{0, d_s N_c, \dots \dots N_s d_s N_c, (N_s d_s + d_n) N_c, \dots \dots, N_c[N_s d_s + (N_n - 1) d_n]\} \tag{12}$$

In this way, if we select $d = 6.25\%$, one period of the BeiDou ranging code is break down into 14 special pulses with duration of 128 chips each and 2 normal pulses with duration of 127 chips each, as illustrated in Figure 2.

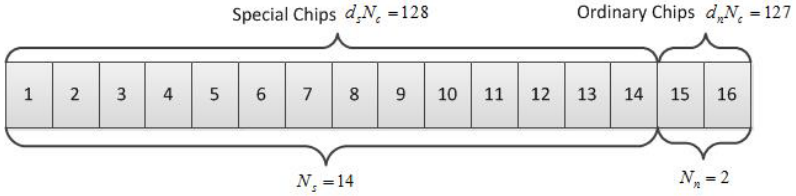

Figure 2: Chip settings of BPL pulsed signal at d=6.25% duty cycle

The second step is to set the order of the transmission time-slots. It can be done by mapping the

ISSN 2616-5872 Vol.6, Issue 5: 12-22, DOI: 10.25236/AJEE.2024.060503

pulse index into the cells from a $N_e \times N_e$ array where the row represents the code period and the column represents the time-slot. In the uniform pulsing scheme, each time-slot occurs once and only once, therefore the order can be defined by a permutation sequence over an alphabet A consisting of m symbols where each symbol exists only once. The permutation sequence can be obtained in either a random or a pseudo-random fashion. For the random fashion, there are possible $N_e! - 2$ permutation sequences can be made, the two exceptions are $(1,2,3, \dots \dots, N_e - 2, N_e - 1, N_e)and(N_e, N_e - 1, N_e - 2, \dots \dots 3, 2, 1)$, because the cyclic shifts are need to be avoided to preserve the spectral properties.

The random permutation sequence is easy to implement and has good spectral properties. However, a significant drawback is that the multi-access performance is relatively low because the signal collision probability arises along with the increase of the BPLs applied in the area. Figure 3 illustrates 4 random pattern arrays for 4 synchronized BPLs at duty cycle $d = 6.25\%$. It can be seen from the figure that collision of two signals occurs three times while three signals are collided in the 16th code period. In order to provide a better multi-access performance, a pseudo-random pattern is preferred to decrease the signal collision probability.

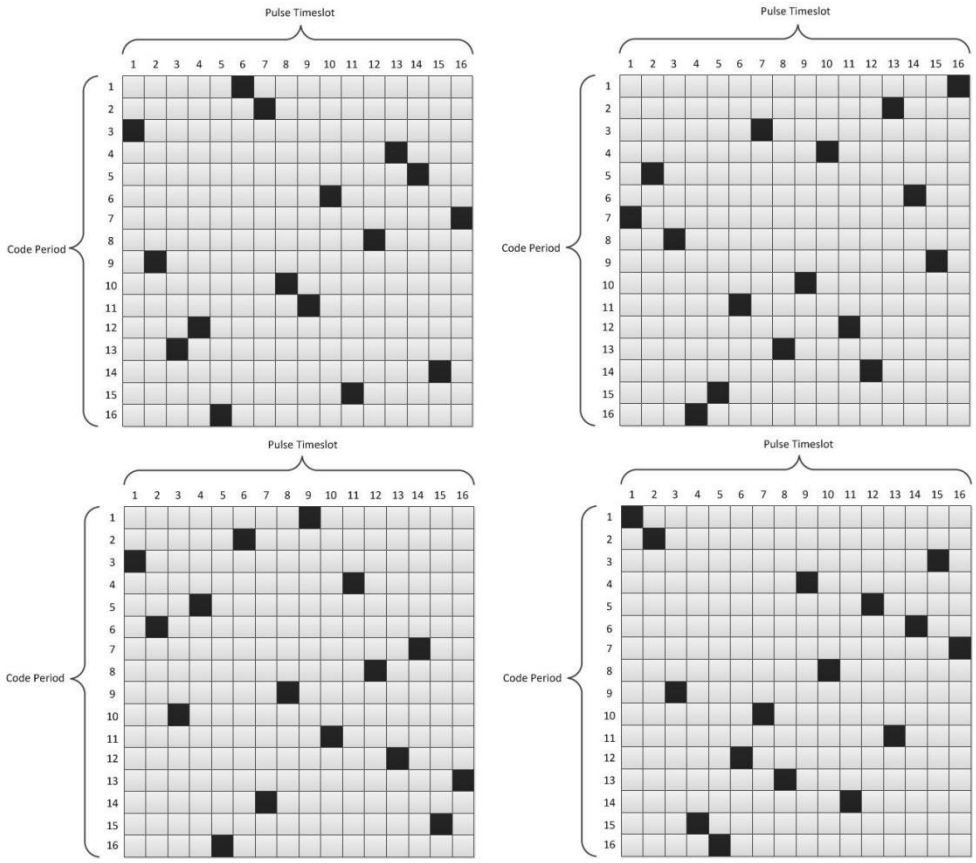

Figure 3: Random pulse pattern with 4 code periods at duty cycle d=6.25%

3.2 Linear congruence pattern

The theory of linear congruence is a widely used pseudo-random permutation sequence generation method in the field of radar and asynchronous spread spectrum communications where the generated sequence possesses most of the desirable properties such as sharp autocorrelation peak and small side-lobs. The pulse pattern considering the linear congruence can be expressed as:

$$k_i(m_i, \tau_i) \equiv m_i \tau_i (mod\ P), 0 \leq m_i, \tau_i \leq P - 1, i = 1,2 \dots \dots, P - 1 \qquad (13)$$

where m_i is the BPL index, k_i is the code period, τ_i is the time-slot and P is a prime number. As an example consider the pattern array generated for $P = 17$ and $i = 16$ shown in Fig. 1. The number inside each cell is the BPL index. It is clear seen from the figure that each BPL index has a unique pattern and for each pattern, each code period and each time-slot occur once and only once. The array contains 16 BPL index, each BPL can possesses 4 different patterns for the 4 synchronized BPLs case.

ISSN 2616-5872 Vol.6, Issue 5: 12-22, DOI: 10.25236/AJEE.2024.060503

Taking P=5 as an example, the remaining classes are {1, 6, -4}, totally {5, 1, 7, -2, 4}, and the absolute minimum full residual is {-2, -1, 0, 1, 2}. When using the linear congruential algorithm, the pseudo-satellite pulse transmission slot generation formula can be expressed as:

$$k_i(m_i, l_i) \equiv m_i l_i (mod\ P), 0 \le m_i, l_i \le P-1, i = 1,2 \dots \dots, P-1 \quad (14)$$

where,k_i is the code period,m_i is the pseudo-satellite number,l_i is the timeslot index,P is an odd prime number. Take the duty cycle d=25%, that is, P=5 as an example

when $l=1, m=1, k=1;\quad m=2, k=2;\quad m=3, k=3;\quad m=4, k=4;$

when $l=2, m=1, k=2;\quad m=2, k=4;\quad m=3, k=1;\quad m=4, k=3;$

when $l=3, m=1, k=3;\quad m=2, k=1;\quad m=3, k=4;\quad m=4, k=2;$

when $l=4, m=1, k=4;\quad m=2, k=3;\quad m=3, k=2;\quad m=4, k=1;$

Similarly, take the duty cycle $d = 6.25\%$, that is $N_e = 16$, in this case $P = 17$, The pulse pattern can be obtained as shown in Figure 4. The figure shows all the 16 pulse patterns. When 4 pseudolites are positioned at the same time, each star can be assigned 4 patterns, which can be reused after 4 modulation cycles.

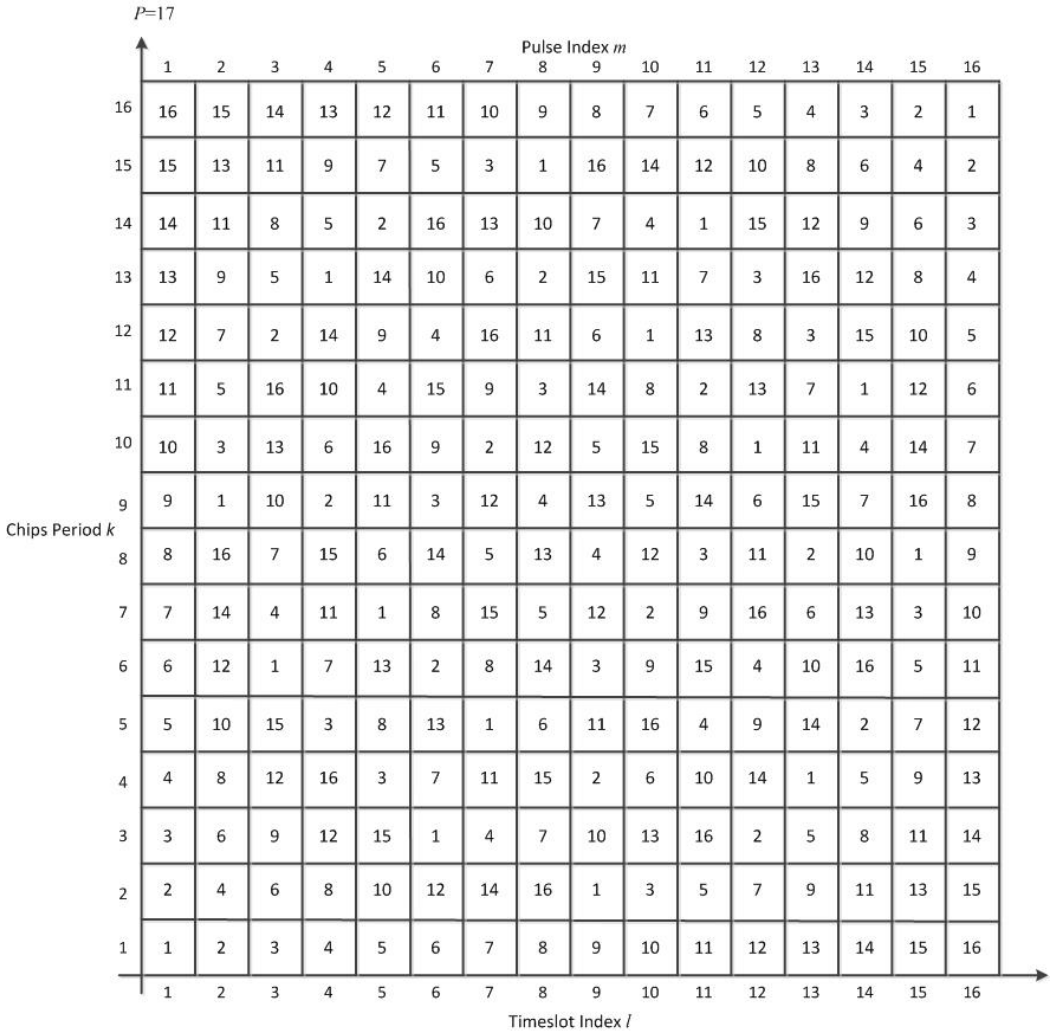

Figure 4: Linear congruence pulse pattern for duty cycle d=6.25%

4. Properties analysis of proposed pulse pattern

Auto-correlation functions and power spectral density are two elementary properties of the pulsed signal. The auto-correlation functions are important to enable initial acquisition of the pulsed signal in the receiver, while the PSD is important to ensure the ranging performance of the pulsed signal is

ISSN 2616-5872 Vol.6, Issue 5: 12-22, DOI: 10.25236/AJEE.2024.060503

similar to that of the original ranging code. In this section, the characteristics of the proposed pulse pattern are determined and compared with the random pulse pattern.

4.1 Auto-correlation functions

The autocorrelation function of the pulse pattern can be expressed as:

$$R_{p\_auto}[l] = \frac{1}{dN_eN_c}\sum_{n=0}^{N_eN_c-1} P_b[n]P_b[n-l] mod\, N_eN_c \tag{15}$$

where l is the shifting operation with the period of N_eN_c. $\frac{1}{dN_eN_c}$ is introduced to have a unit amplitude normalized to one. Using the shifting property of the Kronecker delta $\delta[\cdot]$ and the associative property of convolution, (14) can be rewritten as:

$$R_{p\_auto}[l] = \Lambda_{dN_c}[l] * \left[\frac{1}{N_e}\sum_{n=0}^{N_eN_c-1}\sum_{j=0}^{N_e-1}\sum_{k=0}^{N_e-1}\delta[n-kN_c-\tau_k]\cdot\delta\left[((n-l)modN_eN_c)-jN_c-\tau_j\right]\right] \tag{16}$$

where $\Lambda_{dN_c}[l]$ is obtained by the convolution operation of two rectangular waves:

$$\Lambda_{dN_c}[l] = \frac{1}{dN_c}\Pi_{dN_c}[l] * \Pi_{dN_c}[-l] \tag{17}$$

By exploiting the fact that $\delta[n-kN_c-\tau_k] \neq 0$ when $n = kN_c - \tau_k$, (15) can be written as:

$$R_{p\_auto}[l] = \Lambda_{dN_c}[l] * \left[\frac{1}{N_e}\sum_{j=0}^{N_e-1}\sum_{k=0}^{N_e-1}\delta\left[((\tau_k-kN_c-l)\cdot modN_eN_c)-jN_c-\tau_j\right]\right] \tag{18}$$

Suppose that $N_e \to \infty$, it is possible to obtain the expectation of auto-correlation function of the Dirac delta function by means of approximation

$$,R_{\delta\_auto}[l] \approx \tilde{R}_{\delta\_auto}[l] = \mathrm{E}\left[\sum_{j=0}^{N_e-1}\delta\left[((\tau_k-kN_c-l)\cdot modN_eN_c)-jN_c-\tau_j\right]\right] \tag{19}$$

Using the linearity of the expected value, (18) becomes:

$$\tilde{R}_{\delta\_auto}[l] = \mathrm{P}\left[\sum_{j=0}^{N_e-1}\delta\left[((\tau_k-kN_c-l)\cdot modN_eN_c) = jN_c-\tau_j\right]\right] \tag{20}$$

where $\mathrm{P}[\cdot]$ denotes the probability that the basic pulse pattern equals to its shifting operations. It is noted that the approximation becomes asymptotically exact along with increase of the samples. Then, the autocorrelation function $\tilde{R}_{\delta\_auto}[l]$ can be approximated by averaging the probabilities of several patterns.

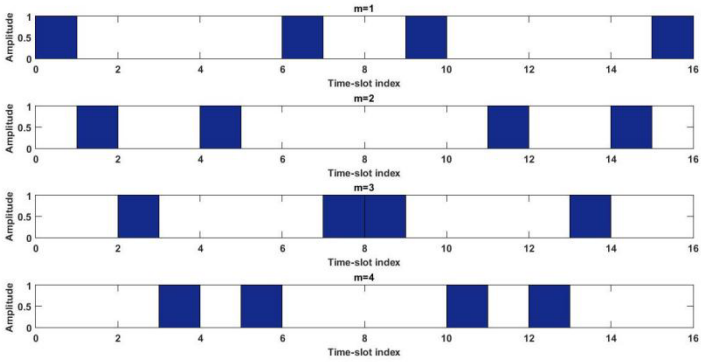

Figure 5: Linear congruence pulse address (P=5)

For $P = 5$, the basic linear congruence patterns for BPL 1~4 are illustrated in Figure 5. According to (17), the average auto-correlation function of 4 basic patterns is shown in Figure 6 where the shifting operation $l = (k * \tau_k) - 1 = 15$ for each pattern. Compared with the random patterns with the same operation, the auto-correlation peaks are nearly identical, and the worst side-slob is $-9.0309\mathrm{dB}$, noticeably lower than $-6.8131\mathrm{dB}$ of the random pattern. $P = 7$ shows the similar results that the worst side slob is $1.25\mathrm{dB}$ smaller than counterpart of the random pattern.

ISSN 2616-5872 Vol.6, Issue 5: 12-22, DOI: 10.25236/AJEE.2024.060503

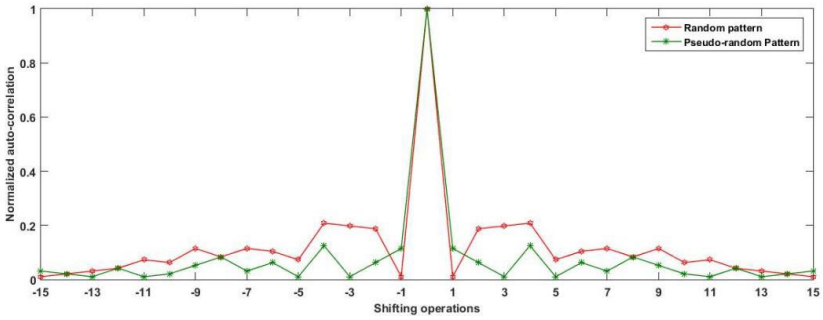

Figure 6: Comparison of autocorrelation function of pulse pattern (P=5)

By averaging $P = 5, 7, 11, 13, 17, 19, 23,$ the expected value of the auto-correlation assumes the following form:

$$\tilde{R}_{\delta\_auto}(l) = \begin{cases} 1, \\ \frac{1}{(N-1)^2}, \\ \frac{2}{(N-2)^2}, \\ 0 \end{cases} \tag{21}$$

the corresponding probabilities are:

$$P_{\delta\_auto}(l) = \begin{cases} \frac{1}{2N-3}, \\ \frac{1}{2N-3}, \\ \frac{N-3}{4N-6}, \\ \frac{3N-7}{4N-6} \end{cases} \tag{22}$$

Figure 7 shows the results of $N = N_e = 16, d = 6.25\%$.

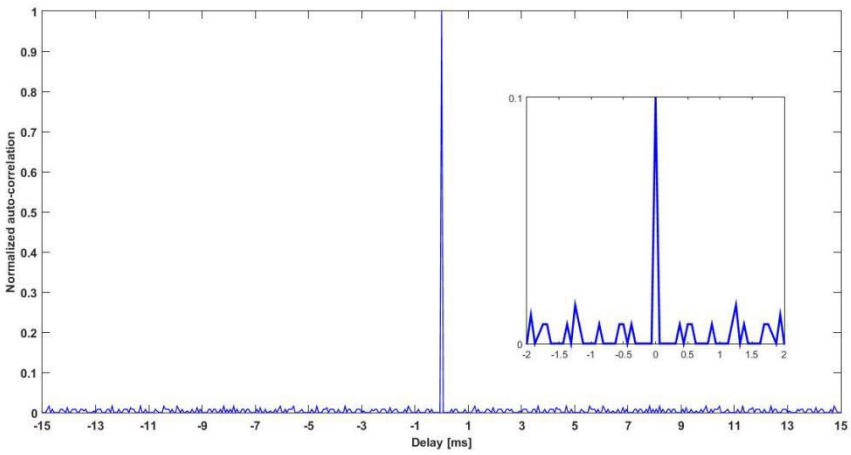

Figure 7: Linear congruence pulse pattern aut0-correlation function (P=17)

4.2 Power spectral density

The PSD of the pulsed signal can be obtained from the Fourier Transform of the autocorrelation function,

$$P(f) = \mathcal{F}\{R_p[l]\} = \sum_{l=-\infty}^{+\infty} R_{p\_auto}[l] exp\{-j2\pi l f T_{ch}\} \tag{23}$$

where T_{ch} is the chip duration, $\mathcal{F}\{\cdot\}$denotes the Discrete Time Fourier Transform.Note that the period of the pulsing scheme is $N_e N_c T_{ch}, P(f)$ can be further expressed in the line spectrum form:

$$P(f) = P_b(f) \cdot \frac{1}{N_e N_c T_{ch}} \sum_{i=-\infty}^{+\infty} \delta\left(f - \frac{i}{N_e N_c T_{ch}}\right) = \frac{1}{N_e N_c T_{ch}} \sum_{i=-\infty}^{+\infty} P_b\left(\frac{i}{N_e N_c T_{ch}}\right) \delta\left(f - \frac{i}{N_e N_c T_{ch}}\right) \tag{24}$$

ISSN 2616-5872 Vol.6, Issue 5: 12-22, DOI: 10.25236/AJEE.2024.060503

where,$P_b(f)$ is the Fourier Transform of the basic pattern:

$$P_b(f) = \sum_{l=0}^{N_eN_c-1} R_{p\_auto}[l]exp\{-j2\pi lfT_{ch}\} \tag{25}$$

Knowing that $R_{\delta\_auto}[l] \approx \tilde{R}_{\delta\_auto}[l]$ when $N_e \gg N$,(24) can be expressed as:

$$P_b(f) \approx \sum_{l=0}^{N_eN_c-1} \tilde{R}_{\delta\_auto}[l]\ exp\{-j2\pi lfT_{ch}\}$$
$$= \mathcal{F}\{\Lambda_{dN_c}[l]\} \cdot \sum_{l=0}^{N_eN_c-1} \tilde{R}_{\delta\_auto}[l]\ exp\{-j2\pi lfT_{ch}\} \tag{26}$$

Inserting (20) and (21) into (25), it can be obtained that

$$P_\delta(f) = \sum_{l=0}^{N_eN_c-1} \tilde{R}_{\delta\_auto}(l) \cdot P_{\delta\_auto}(l)exp\{-j2\pi lfT_{ch}\}$$
$$= \frac{1}{2N-3} + \frac{1}{(N-1)^2(2N-3)} \sum_{l=0}^{N_eN_c-1} exp\{-j2\pi lfT_{ch}\}$$
$$+ \frac{N-3}{(N-1)^2(2N-3)} \sum_{l=0}^{N_eN_c-1} exp\{-j2\pi lfT_{ch}\}$$
$$= \frac{1}{2N-3} + \frac{1}{(N-1)^2(2N-3)} \cdot \frac{1-exp\{-j2\pi N_eN_cfT_{ch}\}}{1-exp\{-j2\pi dN_cfT_{ch}\}} + \frac{N-3}{(N-1)^2(2N-3)}$$
$$\cdot \frac{1-exp\{-j2\pi N_eN_cfT_{ch}\}}{1-exp\{-j2\pi dN_cfT_{ch}\}}$$
$$= \frac{1}{2N-3} + \left[\frac{1}{(N-1)^2(2N-3)} + \frac{N-3}{(N-1)^2(2N-3)}\right] \cdot exp\{-j2\pi dN_c{}^2(N-1)fT_{ch}\} \tag{27}$$

Finally, the PSD $P(f)$ can be obtained by:

$$P(f) = P_b(f) \cdot \frac{1}{T} \sum_{i=-\infty}^{+\infty} \delta\left(f - \frac{i}{T}\right) = \frac{1}{T} \sum_{i=-\infty}^{+\infty} P_b\left(\frac{i}{T}\right) \delta\left(f - \frac{i}{T}\right)$$
$$= \frac{d}{(2N-3)}\delta(f) + (1-\mathrm{d})\left[\frac{1}{(N-1)^2(2N-3)} + \frac{N-3}{(N-1)^2(2N-3)}\right] \cdot \left|\frac{sin(\pi id/N)}{dN_csin(\pi i/NN_c)}\right|^2 \delta\left(f - \frac{i}{T_{ch}}\right) \tag{28}$$

where $dN_c \left|\frac{sin(\pi dN_cfT_{ch})}{dN_csin(\pi fT_{ch})}\right|^2$ is the Fourier Transform of the triangular function $\Lambda_{dN_c}[l]$. The PSD (single side spectrum) of the two patterns is compared. It can be seen from the Figure 8 that the power spectrum side front of the linear congruence pattern is generally smaller than the random pattern, and it has a strong regularity, indicating that the interference in the frequency domain is smaller and easier to eliminate.

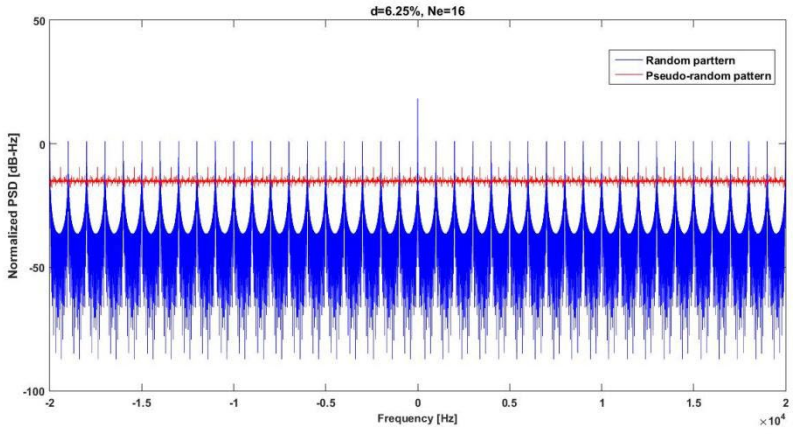

Figure 8: Comparison of power spectral density of pulse patterns

4.3 Multi-access performance

Although the linear congruential pattern is used to transmit the pulse signal, the transmission slots of pseudo-satellite signal do not overlap. But the delay caused by multi-path transmission also may

ISSN 2616-5872 Vol.6, Issue 5: 12-22, DOI: 10.25236/AJEE.2024.060503

generate a certain signal collision and generate cross-correlation interference, so the cross-correlation function of the pulse pattern determined its multiple access performance. The solving process of cross-correlation function is similar to that of the autocorrelation function. First, taking cross-correlation operation from the initial pulse pattern in Figure.9. The resulting cross-correlation operation result is shown in Fig.. Then calculating the signal collision probability at $P = 7,11,13,17,19$in turn and performing statistics, the average cross-correlation function can be calculated as:

$$R_{\delta\_auto}[l] = \frac{1}{m}\sum_{i,j,i\neq j}^{m} E(S_i)\,E(S_j - l) = \frac{(N-1)^2}{[2(N-1)^2-1]^2} \tag{29}$$

Where S_k is the m pulse code-word index, $S = \{S_1, S_2, \cdots, S_k, \cdots, S_l\}$, $K = N! - 1$ are all lobes. The average value of cross-correlation function about the random pattern in the reference is $1/N$. When $P = 17$, the cross-correlation value of the linear congruence pattern is -53.8925dB, and the cross-correlation value of the random pattern is -27.72dB.

Assuming there are three interference signals, like the target signal, the power is -90dBm, and the duty ratio is $d = 6.25\%$. Comparing the simulation results of the acquisition probability between random pattern and linear congruence pattern. It has known that false alarm probability is $P_{fa} = 0.1\%$, non-coherent integration time is1ms, the number of coherent integrations is 25, Figure 10 shows the detection probability curve ofC/N_0 changing from 60dB$\cdot$Hz to 110dB$\cdot$Hz. When the signal C/N_0s 80dB$\cdot$Hz, the capture probability of the linear congruential pattern is 74.44%, and the capture probability of the random pattern is 16.24%. This result can prove that in the case of the same receiver setup and interference, the multi-access performance of linear congruent pattern is better.

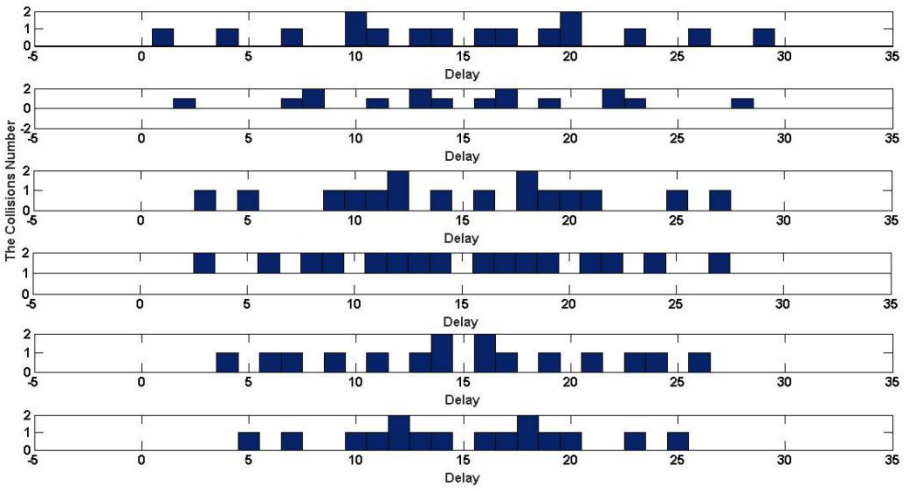

Figure 9: Linear Congruence Pulse Pattern Cross-Correlation Calculation Results (P=5)

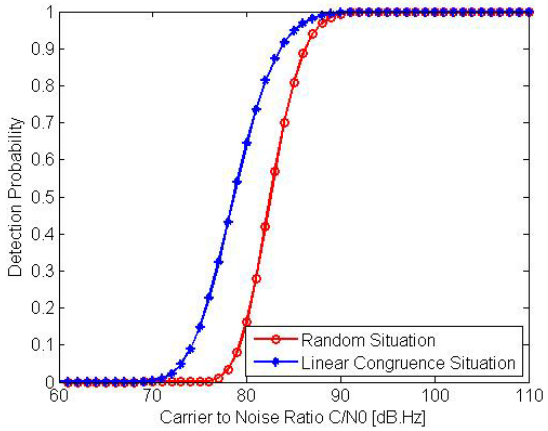

Figure 10: Pulse signal acquisition probability curve under three-way interference

ISSN 2616-5872 Vol.6, Issue 5: 12-22, DOI: 10.25236/AJEE.2024.060503

4.4 Singal spacing

The spacing of BPLs is determined by the interval between transmissions of the pulses. Assuming that the receiver receives the signals of the pseudolites A and B at the same time, the duty ratio is $d = 6.25\%$. At a certain moment, the transmission slot of the pseudolite A is 5, the transmission slot of the pseudolite B is 8, and the phase difference is 3 time slots. At this time, if the receiver distance A is 18.75 kilometers and the distance B is 90 kilometers, the signals A and B will be simultaneously received, that is, the signal will collide. Therefore, the minimum distance should be larger by one time difference τ than the time interval, so as to avoid the collision of two or more signals. In this paper, the random pattern of 10000 pulse modulation periods and the slot spacing of linear congruential patterns are counted. The probability density function is shown in Figure 11. The mean time slot spacing of the random pattern is 0.35ms, and the linear congruence is 0.3ms. Therefore, the minimum distance of linear congruential patterns is 15 km smaller than that of the random pattern, that is, the distance between two BPLs can be reduced about 15 kilometers.

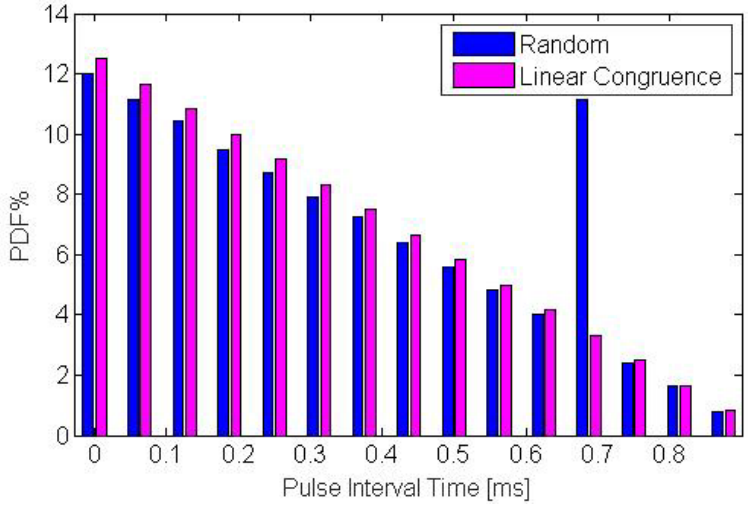

Figure 11: Comparison of pulse pattern signal spacing probability density

According to the analysis and comparison of the above characteristics, the correlation characteristics, power spectral density and signal spacing of the linear congruential pulse pattern are better than the random pattern, and have better acquisition performance and shorter receiver spacing.

5. Conclusion

This paper studies and designs the BPL signal pulse modulation scheme. Firstly, the signal pulse modulation model is established, and the design requirements of the two most important parameters in the model, the duty cycle and the pulse pattern are analyzed. Then, the partial correlation characteristics of BPL signals are analyzed, and a relation model of partial correlation characteristics and signal acquisition is established. When the probability of capture is 99.9% and the number of interference signals is 6, the minimum value of duty cycle should be 6.25%, so set the duty cycle of the pulse modulation scheme to 6.25%. Five BPLs can be deployed with an ordinary receiver.

Aiming at the shortcomings of random pattern signals with high collision probability, a pseudo-random pulse pattern design scheme based on linear congruential algorithm is proposed, and the signal correlation function, power spectral density, multiple access performance and signal spacing of the scheme are performed. Analyzed and compared. Simulation results show that this scheme satisfies the design requirements and the signal characteristics are better than random patterns. The scheme has been adopted by the project group of the “Key Technology of BeiDou Ground-Based Navigation Signal Network” project of the 863 project and applied to the pseudo-satellite signal design, and further testing and analysis has been conducted.

ISSN 2616-5872 Vol.6, Issue 5: 12-22, DOI: 10.25236/AJEE.2024.060503

Acknowledgements

This work was financially supported by the President's Fund of Guangdong Environmental Protection Engineering Vocational College (K620822062406): Research on a Grid based Smart Service Platform for Marine Ranch Geoenvironmental Data in the Guangdong Hong Kong Macao Greater Bay Area.

References

[1] Kang G, Tan L, Hua B, et al. Study on Pseudolite System for BeiDou Based on Dynamic and Independent Aircrafts Configuration[J]. Lecture Notes in Electrical Engineering, 2013. 244: 159-172.
[2] Zhu G, Huang K. Analog Spatial Cancellation for Tackling the Near-Far Problem in Wirelessly Powered Communications[J]. IEEE Journal on Selected Areas in Communications, 2015. PP(99): 1.
[3] Wellens M, Mahonen P. Lessons learned from an extensive spectrum occupancy measurement campaign and a stochastic duty cycle model[J]. Mobile Networks & Applications, 2010.15(3): 461-474.
[4] Li L, Townsend J K. Near-Far Resistant Synchronization for UWB Communications[J]. IEEE Transactions on Wireless Communications, 2011.10(2): 519-529.
[5] Jin Y S, Jeon S G, Kim G J, et al. Fast scanning of a pulsed terahertz signal using an oscillating optical delay line.[J]. Review of Scientific Instruments, 2007.78(2): 721.
[6] Yao K, Ruan X, Mao X, et al. Variable-Duty-Cycle Control to Achieve High Input Power Factor for DCM Boost PFC Converter[J]. IEEE Transactions on Industrial Electronics, 2011.58(5): 1856-1865.
[7] Bibak K, Kapron B M, Srinivasan V, et al. Restricted linear congruences[J]. Journal of Number Theory, 2017. 171: 128-144.
[8] Markoll R. Portable applicator for pulsed signal therapy[Z]. U.S. Patent 7,785,245. 2010.